Comprehensive Modulation of Naphthopyran Photochromism in a Rigid Host Matrix by Applying Polymer Conjugation

Francesca Ercole,[†,‡,§] Thomas P. Davis,[§] and Richard A. Evans*[,†,‡,§]

CSIRO Molecular & Health Technologies, Bag 10, Clayton VIC 3169 Australia, The Cooperative Research Centre for Polymers, 8 Redwood Drive, Notting Hill, VIC 3168, Australia, and Centre for Advanced Macromolecular Design, School of Chemical Sciences and Engineering, The University of New South Wales, Sydney, NSW 2052, Australia

Received August 28, 2008; Revised Manuscript Received December 11, 2008

ABSTRACT: Naphthopyran polymer conjugates of various rigidities were synthesized by atom transfer radical polymerization (ATRP), and their photochromic properties were tested within a rigid host matrix. Broad tuning of photochromic kinetics was displayed as a result of polymer conjugation because of its ability to alter the local environment of the naphthopyran within the host. End-functionalized conjugates, synthesized from a naphthopyran-functionalized ATRP initiator, allowed systematic tuning of kinetics via modulation of chain length of attached polymer. Reducing the rigidity of the conjugate resulted in an acceleration of kinetics and an increase in colorability. Pronounced chain lengths of poly(methyl methacrylate) (>18 000 g/mol) were required for decoloration kinetics to be effectively depressed compared with an unconjugated naphthopyran control. Random in-chain incorporation of the naphthopyran was afforded by copolymers made with naphthopyran-functionalized monomers. At the expense of a defined placement of the dye moiety with respect to the conjugated polymer chain, such conjugates displayed a pronounced ability to influence the kinetics. Persistent color due to thermally stable isomer populations was observed for all samples and found to be uninfluenced by polymer conjugation.

Introduction

The increasing interdisciplinary interest in photochromic materials in the last two decades has been a recognition of their practical as well as potential applications in a number of areas such as ophthalmic lenses, optical switches, optical filters, and temporary or permanent memory devices, to name several.[1−5] The regulation of the photochromic response, seen as a reversible color change, is always of primary importance. However, a recent focus has also been the use of photochromism to control other properties of the material such as self-assembly and fluorescence simultaneously.[6−10] Common to many of these new photochromic applications is the use of engineered polymers.

A group of photochromic molecules that has received considerable attention in industry are chromenes (benzopyrans) and the related naphthopyrans.[11−13] UV irradiation of the colorless photochromic results in the electrocyclic ring opening of the pyran moiety via the cleavage of the C(sp^3)−O bond. This produces a distribution of isomeric open forms (merocyanines) that are intensely colored because of their extended conjugation and quasi-planar conformations. Comprehensive NMR and time-resolved spectroscopy studies have underlined the formation of two main classes of transoid open structures, namely, trans−cis (TC) and trans−trans (TT) geometrical isomers. These colored isomers dominate the kinetics and gradually thermally or photochemically electrocyclize back to the original closed benzo/naphthopyran form. For the conversion from the closed to open form to take place, the molecules must undergo a large intramolecular rotation, as shown in Scheme 1.[14−17]

The use of diaryl-naphthopyrans in sun-protective ophthalmic lenses remains by a wide margin their largest practical and commercial application. Their chemistry has been intensely studied, and increasingly complex derivatives with additional substituents and fusion to different heterocyclic systems have been developed to modulate their photochromic behavior and enhance their performance.[18−26] Properties that are important include the ability to produce colored forms, maxima wavelengths of absorption, resistance to photodegradation, and modulation of fading kinetics.

Scheme 1. Photochromic Isomerizations of Substituted 2,2-Diaryl-2*H*-naphtho[1,2-*b*]pyran[a]

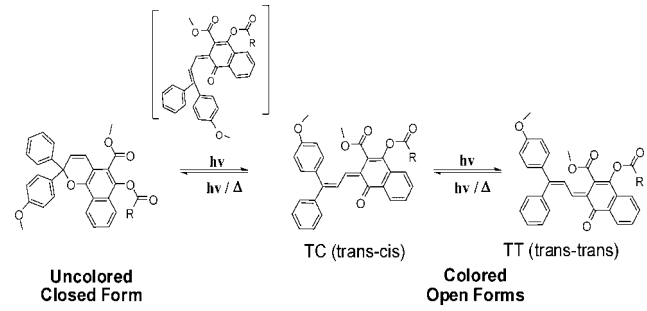

[a] Asymmetry at quaternary carbon results in four isomers: CTC (shown), TTT (shown), TTC, and CTT.

The photochemical and thermal de/coloration behaviors of the molecules are profoundly influenced by the media that incorporates them. In a rigid, optically clear matrix, maintaining and controlling photochromic switching ability is a challenge; rigidity, viscosity, and free volume imparted by the local host environment are major influencing factors.[27−29] Efforts aimed at chemically developing dyes with predictable responses have been impressive; however, those characteristics that are displayed in solution are rarely consistently replicable in a solid matrix. The strategic design of optically viable host materials that both impart stringent mechanical requirements and preserve the switching capacity of the photochromic remains a challenge. Both approaches have obvious limitations, especially for multidye ophthalmic systems in which the transitions of multiple dyes need to be synchronized and therefore controlled for the system to display desirable color evolutions.

* Corresponding author. E-mail: richard.evans@csiro.au (R.A.E.).
† CSIRO Molecular & Health Technologies.
‡ The Cooperative Research Centre for Polymers.
§ The University of New South Wales.

10.1021/ma801947d CCC: $40.75
Published on Web 02/10/2009

A strategy developed in our laboratory that has provided control and greater predictability over the photochromic behavior is the use of polymer conjugation. The aim is to control kinetics effectively by neither modifying the electronic structure of the dye nor by modifying an optimized host matrix, but instead by affecting the local environment in the vicinity of the photochromic molecule. When incorporated within a host matrix, as used for ophthalmic lens and optical applications, entanglement and partitioning of polymer tails around covalently attached photochromic molecules creates, to varying degrees, a level of encapsulation and insulation from the bulk environment. The local environment can therefore be rationally defined by the choice of attached polymer.

To introduce polymer conjugation, controlled radical polymerization techniques are indispensable. By using techniques such as atom transfer radical polymerization (ATRP)[30] or reversible addition−fragmentation chain transfer (RAFT)[31,32] polymerization, polymers with defined architectures and functionalities can be accessed with controlled molecular weights (M_n and M_w) and polydispersities (PDI = M_w/M_n) and hence with adjustable compositions and properties. Aspects such as the ability of the architecture, composition, and chain length of the attached polymer to impart a specific response to several photochromic classes continue to motivate our research efforts.[5,33−40] Since our initial report exemplifying the utility of the methodology,[36] other researchers have also successfully applied controlled radical polymerization techniques to their photochromic systems.[10,41]

The techniques can be exploited by growing a polymer from a dye-functionalized radical initiator so that each photochromic moiety will be covalently bound to the end of a similar polymer chain.[36−39] The ability of the polymer conjugation to modify photochromic behavior can be practically examined by variation of chain length and chain composition. Recent advances within our research group have also examined architectural modifications (end placement of the dye vs midplacement) to enhance and tune speed and impart higher colorability.[40]

Our research has reported the thermal decoloration behavior of a spirooxazine dye[5,36−39] in a range of environments. 2,2-Diphenyl-2*H*-naphtho[1,2-*b*]pyrans, widely known as chromenes, are pertinent photochromic dyes because of their excellent photochromic properties and commercial significance.[42] Global studies related to these heterocyclic dyes continue to concentrate on synthetic aspects[11,13,43−46] and their photophysical behavior in solution.[45,47,48] Their bulky substitution patterns suggest a large impact from their local environment; however, investigations regarding their behavior within polymers remain limited.[40,41]

In this work, ATRP techniques were used to introduce polymer conjugation to investigate the influence of the local environment on the photochromic behavior of a 2,2-diphenyl-2*H*-naphtho[1,2-*b*]pyran dye from the rigid local environment imparted by conjugation to high T_g (glass-transition temperature) methacrylates, poly(methyl methacrylate) (pMMA) and poly(carbazolyl ethyl methacrylate) (pCEM), to the fluidlike local environment provided by poly(2-ethylhexyl acrylate) (pEHA).

The ability of polymer conjugation to dominate kinetic responses and influence colorability as well as the capacity of the host matrix to incorporate the broad ranging conjugates without loss of optical clarity was presented. In addition, how profoundly the photochromic kinetics could be affected by the placement of the dye in the chain (in vs at the end) was examined by the evaluation of naphthopyran copolymer conjugates. All aspects were investigated with a view toward optimizing future architectures and conjugate compositions.

Results and Discussion

To synthesize our photochromic conjugates, the preliminary requirement was a naphthopyran with a free hydroxyl group that could be made in sufficient yield for the survey. This was satisfied by the patented naphthopyran dye, **1**.[49] The red-coloring derivatives, **3**−**5**, which are required for the polymerizations, and the isobutyrate control, **2**, were then easily prepared from the base hydroxyl naphthopyran **1** via simple esterification routes, as shown in Schemes 2 and 3.

Polymerization: Conjugate Synthesis

A series of naphthopyran conjugates, p(EHA), p(MMA), and p(CEM), of increasing molecular weight and of various inherent rigidity were first produced (Scheme 2) using ATRP initiator **3**. Then, correspondingly for each polymer type, a random copolymer comparison was also produced, as in Scheme 3, using the naphthopyran comonomers, **4** and **5**. Both methodologies necessarily produce naphthopyran−polymer conjugates via ATRP but are distinct from one another from the point of view of where the naphthopyran resides in the final polymer chains: the first precisely places the dye at the end of each polymer chain in comparison with the second methodology that randomly incorporates the naphthopyran moieties in the chains (in-chain vs end-of chain). All conjugates were compared with the electronically equivalent isobutyrate control **2** that, by not having the polymer attached, allows the effect of the conjugation to be displayed.

The ATRP polymerizations of the end-functionalized naphthopyran conjugates were monitored to gauge the viability of ATRP conditions and then applied to generate the corresponding copolymer samples.

The EHA polymerizations were carried out using CuBr and the 4,4′-dinonyl-2,2′-bipyridine (dNbpy) catalyst system at 90 °C. Polymerizations proceeded effectively with low PDIs throughout and with only minor deviations from expected molecular weight (Figure 1, evolution plot). Furthermore, the first-order kinetics plot displayed a near-linear relation with time. (See the Supporting Information.)

MMA polymerizations were carried out using a Haddleton ligand, *N*-(*n*-pentyl)-2-pyridylmethanimine (*N*-PPMA),[50] and CuBr in toluene at 90 °C. As shown by the pMMA evolution plot (Figure 2), the ATRP polymerization proceeded well with molecular weights (M_n) increasing linearly with conversion, even up to >90%, so that samples with even higher M_n values could be accessed. The first-order kinetics plot showed linearity up until such high conversions with a brief induction period at the beginning of the polymerization. (See the Supporting Information.)

The CEM polymerizations (Figure 3) proved to be more challenging. Using the *N*-PPMA/CuBr catalyst system, the polymerization was initially slow, yet it still showed a controlled growth with time. However, the first-order kinetics plot clearly shows that after 5 h of slow polymerization, the rate of polymerization dramatically changed to give higher conversions (>60%) and broadened PDIs (>1.3). (See the Supporting Information.) It is believed that the reduced solubility that was observed at this point resulted in an inhomogeneous monomer distribution and nonlinear rate of polymerization with time. In any case, we found that samples that were prepared from these pCEM conjugates with higher M_n values (>14 000 g/mol) could not be used for photochromic testing because of the lack of optical clarity of their ensuing test samples. To access samples with molecular weights between these limits (>5400 and <14 000 g/mol), another CEM polymerization trial was carried out with a more active catalyst system that supplied more desirable samples of M_n = 10 600 and 12 100 g/mol during the polymerization time, albeit with slightly higher polydispersities.

Scheme 2. Atom Transfer Radical Polymerization Synthesis of Naphthopyran End-Functionalized Conjugates[a]

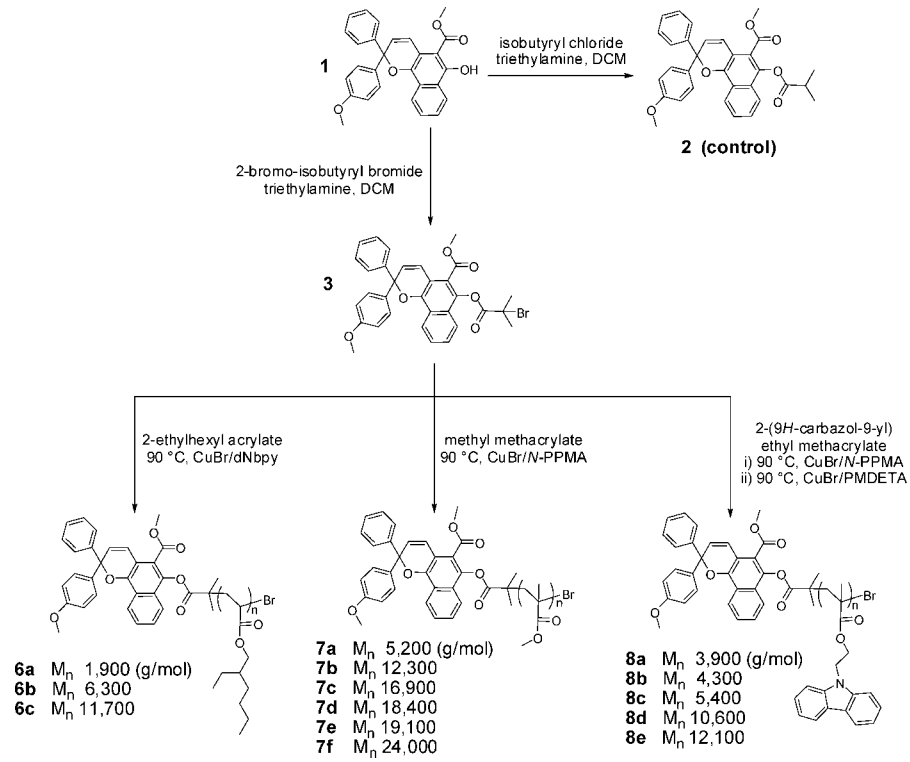

[a] dNbpy: 4,4′-dinonyl-2,2′-bipyridine, *N*-PPMA: *N*-(*n*-pentyl)-2-pyridylmethanimine, PMDETA: *N*,*N*,*N*′,*N*′,*N*″-pentamethyldiethylenetriamine.

The composition and M_n of the copolymer samples **9**−**11**, shown in Scheme 3, were determined by ^{1}H NMR and GPC, respectively. Because the polymers had M_n values similar to those of corresponding end-functionalized conjugates (**7b**, **8d**, and **6c**), these provided insightful comparisons for assessing the effect of dye location on photochromic kinetics. Assigned ^{1}H NMR spectra have been included in the Supporting Information for reference. The polymerization characteristics of all tested naphthopyran polymer conjugates are shown in Table 1.

Optical Clarity of Test Samples. Photochromic test samples were prepared by adding the photochromic conjugates (and control **2**) individually to a lens monomer formulation at a set concentration level (1.5×10^{-7} mol/g host matrix composition for the end-functionalized conjugates). This was composed of poly(ethylene glycol) 400 dimethacrylate (PEGDMA) and 2,2′-bis(4-methacryloxyethoxy)phenyl propane (EBPDMA) (1:4 weight ratio) with 0.4% by mass azobis(isobutyronitrile) (AIBN). The formulations were thoroughly mixed and thermally cured in a mold to produce optically clear test samples (as described in the Experimental Details).

It is envisaged that as the host material polymerizes to form the bulk matrix during the curing process, the polymer attached to the photochromic moiety coils and entangles to varying degrees around the dye molecules and their aggregates. The technique therefore aims to regulate the photochromic response as a result of the interactions of the dye with the polymer. From the perspective of the dye molecule, the conjugation creates an overall pseudoencapsulation effect. In addition to this general description, the formation of distinct phases or domains within the host, containing collections or clusters of multiple photochromic polymer conjugates, is a possibility but remains difficult to determine, especially considering that the doping levels required for the ophthalmic materials are considerably low. Nonetheless, these domains, if formed as distinct phases, need to be confined to the nanoscale (ca. <200 nm) for samples to be optically transparent (i.e., not cloudy/hazy) and to refrain from causing interference with optical testing. Whereas reducing the miscibility of the polymer tail with the host will intuitively act to promote encapsulation of attached dye molecules, it must also be kept to a level that does not cause gross and visibly obvious phase separation. The requirement for successful incorporation of photochromic conjugates within the host is therefore the optical clarity of ensuing test samples.

Within this investigation, several conjugate types were tested. It was found that all pMMA conjugates (**7a**−**7f** and **9**) of a broad M_n range (up to 24 000 g/mol) could be incorporated into the host matrix at the desired concentration level. This was also the case for the pCEM conjugates (**8a**−**8e** and **10**). Out of the pEHA conjugates synthesized, only the lower M_n conjugates (**6a** and **6b**) could be successfully incorporated into the host at the desired concentration level. Samples **6c** and **11** displayed mild phase separation and were therefore doped at half of the concentration to allow testing.

It is apparent that the chemical composition, chain length of the polymer conjugate, and concentration within the host are all associated factors that affect successful incorporation. Such aspects will continue to be monitored in future investigations.

Photochromic Kinetics. The thermal decoloration of the naphthopyran test samples was investigated in the dark at 20 °C after continuous UV irradiation. As depicted in Scheme 1, exposure of the original closed form (CF) to continuous UV light irradiation results in the establishment of a photosteady state made up of an equilibrium distribution of colored merocyanine isomers, which are displayed as a leveling of the absorbance value (optical density) in the coloration curve. The two main classes of merocyanine isomers (transoid cis (TC) and transoid trans (TT)) are produced in consecutive steps and have similar absorption spectra but different thermodynamic stabilities and activation properties (enthalpies and entropies) for isomerization, as shown by NMR studies over the past decade.[14−16]

Scheme 3. Atom Transfer Radical Polymerization Synthesis of Napthopran Random Copolymer Conjugates[a]

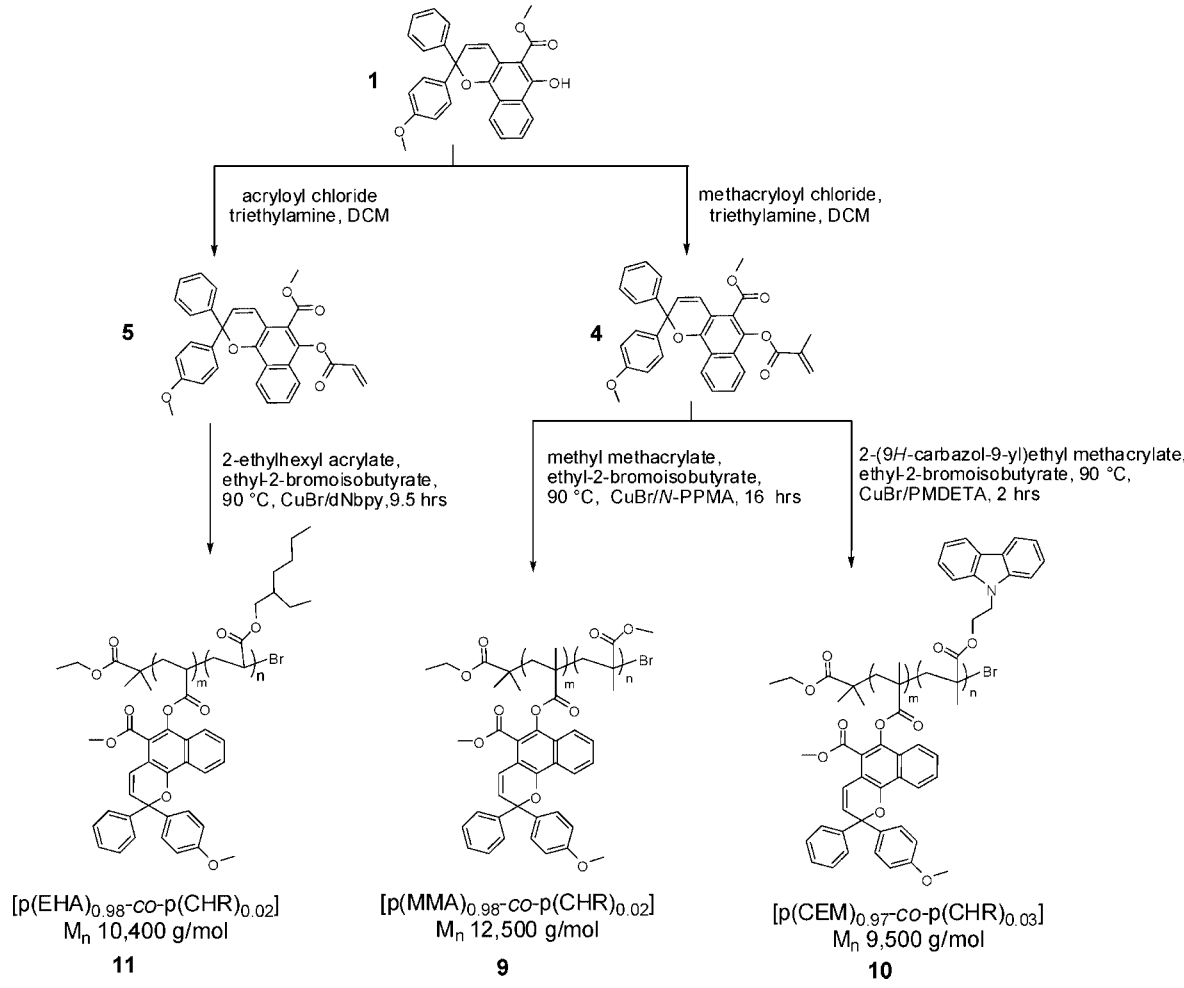

[a] CHR refers to naphthopyran monomer, dNbpy: 4,4′-dinonyl-2,2′-bipyridine, *N*-PPMA: *N*-(*n*-pentyl)-2-pyridylmethanimine, PMDETA: *N*,*N*,*N*′,*N*′,*N*″-pentamethyldiethylenetriamine.

As an example, Figure 4 shows the absorption profile of the control naphthopyran dye **2** before and after UV exposure. The photochromic kinetics of the naphthopyran samples was studied by monitoring the open forms' maximum absorption wavelength with time. The following empirical equation[16,51] was used to analyze and compare the thermal ring closure kinetics (thermal bleaching/decoloration) of the photochromic test samples

$$A(t) = A_1 e^{-k_1 t} + A_2 e^{-k_2 t} + A_{th} \quad (1)$$

where A(t) is the optical density at λ_{max} of the open forms; A_1 and A_2 are the contributions to the initial optical density, A_0; k_1 and k_2 are exponential decay rate constants of fast and slow components, respectively; and A_{th} is the residual coloration (offset) at the termination of the testing time. Simple exponential decoloration behavior in solution (either biexponential or monoexponential with a residual term) can be attributed to the two main classes of colored merocyanines decaying with disparate first-order rate constants. Within solid matrices, distributions of environments, such as free volume, as opposed to the monodisperse environment of a solution, can also account for variations in kinetics. Therefore, the separated constants, k_1 and k_2, in the equation above, along with their allocated contributions to initial optical density, are understood as overall empirical values between notable fast and slow kinetic components. The equation was previously used to represent and compare the decoloration behavior of both spirooxazines and naphthopyrans within solid media[41,51,52] and has consistently fit our decoloration curves with correlation coefficients (R) of greater that 0.99.[36,38−40] Measured $t_{1/2}$ values (time to fade to half of the initial absorbance value) are also beneficial for comparing overall kinetics. The kinetic data for the thermal

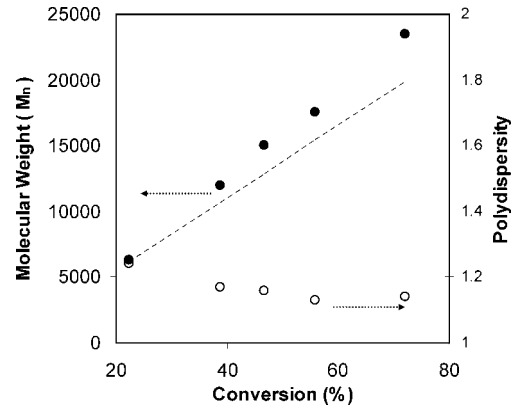

Figure 1. Evolution of polydispersity (○) and molecular weight (●) with conversion for the atom transfer radical polymerization of 2-(ethylhexyl acrylate) at 90 °C in bulk where [monomer]/[CuBr]/[4,4′-dinonyl-2,2′-bipyridine]/[3] = 150:1:2:1. Calculated molecular weight (----) by NMR conversion using the equation M_n = ((monomer MW)([monomer]/[**3**])(NMR conversion)) + (MW of **3**). Polymerization times ranged from 1 to 7 h.

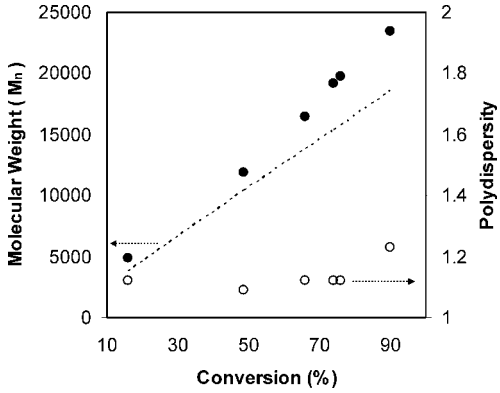

Figure 2. Evolution of polydispersity (○) and molecular weight (●) with conversion for the atom transfer radical polymerization of methyl methacrylate at 90 °C in toluene where [monomer]/[CuBr]/[*N*-(*n*-pentyl)-2-pyridylmethanimine]/[**3**] = 200:1:2:1. Calculated molecular weight (----) by NMR conversion using the equation M_n = ((monomer MW)([monomer]/[**3**])(NMR conversion)) + (MW of **3**). Polymerization times ranged from 2 to 16 h.

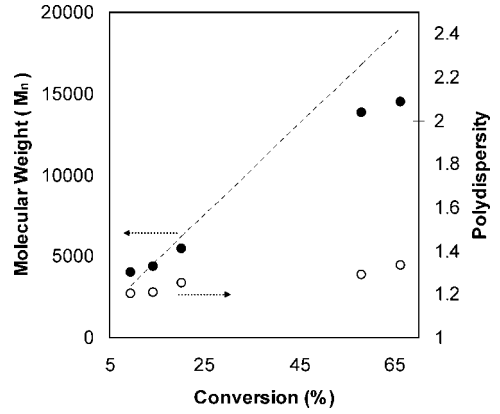

Figure 3. Evolution of polydispersity (○) and molecular weight (●) with conversion for the atom transfer radical polymerization of 2-(9*H*-carbazol-9-yl)ethyl methacrylate at 90 °C in toluene where [monomer]/[CuBr]/[*N*-(*n*-pentyl)-2-pyridylmethanimine]/[**3**] = 100:1:2:1. Calculated molecular weight (----) by NMR using the equation M_n = ((monomer MW)([monomer]/[**3**])(NMR conversion)) + (MW of **3**). Polymerization times ranged from 3 to 6 h.

decoloration of all naphthopyran conjugate test samples and the control dye **2** are shown in Tables 2 and 3.

Tuning of Thermal Decoloration Rate: Chain Length and Rigidity Affects. The kinetic survey of naphthopyran conjugates commenced with a brief review of the decoloration performance of the low T_g pEHA conjugates that could be incorporated into the host matrix and a comparison of their behavior with that of the control dye **2** in solution as well as in the matrix (Table 2 and Figure 5). As in solution, all of the samples tested (including the high T_g conjugates described below) produced a persistent colored isomer population with normalized decoloration curves converging to similar residual values (A_{th}). It was found that as with many other chromene/naphthopyran dyes this isomer population could be fully removed only photochemically with exposure to visible irradiation and can be attributed to more thermally stable TT-type isomers.[14]

As expected, the low T_g conjugates displayed accelerated switching speeds in the rigid host matrix with respect to control **2** (Figure 5). This was apparent even for the lower M_n value (<2000 g/mol, **6a**), and the modestly higher M_n of 6300 g/mol, **6b**, elicited a profound effect that closely approached the behavior of the control in solution (Figure 5, $t_{1/2}$ value of 63 s for **2** in toluene vs 70 s for conjugate **6b** in the matrix). In previous investigations using *n*-butyl acrylate-naphthopyran[40] and spirooxazine[38] end-functionalized conjugates, higher M_n

Table 1. Polymerization Characteristics of Naphthopyran Dye Conjugates (Refer to Schemes 2 and 3)

sample	time (min)[a]	conv. (%)[b]	exptl M_n[c]	theor M_n[d]	PDI
6a	60	7	1900	1880	1.08
6b	60	22	6300	6165	1.24
6c	120	39	12 000	10 700	1.17
7a	120	16	4900	3790	1.12
7b	240	49	11 800	10 300	1.09
7c	370	66	16 400	13 800	1.12
7d	480	74	19 200	15 400	1.12
7e	540	76	19 800	15 805	1.12
7f	960	90	23 500	18 610	1.23
8a	180	9	4000	3210	1.20
8b	240	14	4300	4580	1.21
8c	300	20	5400	6240	1.25
8d	90	60	10 600	17 350	1.27
8e	180	76	12 100	21 820	1.27
9[e]	960	70	12 500	15 350	1.29
10[e]	120	63	9500	17 650	1.27
11[e]	570	50	10 400	9532	1.12

[a] Polymerization for **6a** performed with 2-(ethylhexyl acrylate) at 90 °C in bulk where [monomer]/[CuBr]/[4,4′-dinonyl-2-2′-bipyridine]/[**3**] = 100:1:2:1; polymerizations for **6b** and **6c** performed with 2-(ethylhexyl acrylate) at 90 °C in bulk where [monomer]/[CuBr]/[4,4′-dinonyl-2-2′-bipyridine]/[**3**] = 150:1:2:1; polymerizations for **7a-7f** were performed with methyl methacrylate at 90 °C in toluene where [monomer]/[CuBr]/[*N*-(*n*-pentyl)-2-pyridylmethanimine]/[**3**] = 200:1:2:1; polymerizations for **8a-8c** performed with 2-(9*H*-carbazol-9-yl)ethyl methacrylate at 90 °C in toluene where [monomer]/[CuBr]/[*N*-(*n*-pentyl)-2-pyridylmethanimine]/[**3**] = 100:1:2:1; polymerizations for **8d** and **8e** performed with 2-(9*H*-carbazol-9-yl)ethyl methacrylate at 90 °C in toluene where [monomer]/[CuBr]/[*N,N,N′,N′,N″*-pentamethyldiethylenetriamine]/[**3**] = 100:1:1:1; polymerization for **9** performed with methyl methacrylate and **4** (98:2 molar ratio) at 90 °C in toluene where [monomers]/[CuBr]/[*N*-(*n*-pentyl)-2-pyridylmethanimine]/[ethyl-2-bromoisobutyrate] = 200:1:2:1; polymerization for **10** performed with 2-(9*H*-carbazol-9-yl)ethyl methacrylate and **4** (94:6 molar ratio) at 90 °C in toluene where [monomers]/[CuBr]/[*N,N,N′,N′,N″*-pentamethyldiethylenetriamine/[ethyl-2-bromoisobutyrate] = 100:1:1:1; polymerization for **11** performed with 2-(ethylhexyl acrylate) and **5** (97:3 molar ratio) at 90 °C in toluene where [monomers]/[CuBr]/[4,4′-dinonyl-2-2′-bipyridine]/[ethyl-2-bromoisobutyrate] = 100:1:2:1. [b] Determined by ^{1}H NMR analysis of polymerization mixture. [c] Determined by GPC with THF as eluent: for **6a**−**6c** and **11**, poly(2-ethylhexyl acrylate) equivalents were obtained using Mark-Howink parameters on a PS calibration; for **7a**−**7f** and **9,** calibration with pMMA standards; for **8a**−**8e** and **10**, PS standards used for calibration. [d] Calculated on the basis of monomer conversion plus initiator molecular weight. [e] Final composition of copolymers estimated by integration ratios of napthopyran proton versus that of comonomer. Final compositions shown in Scheme 3; ^{1}H NMR images displayed in the Supporting Information.

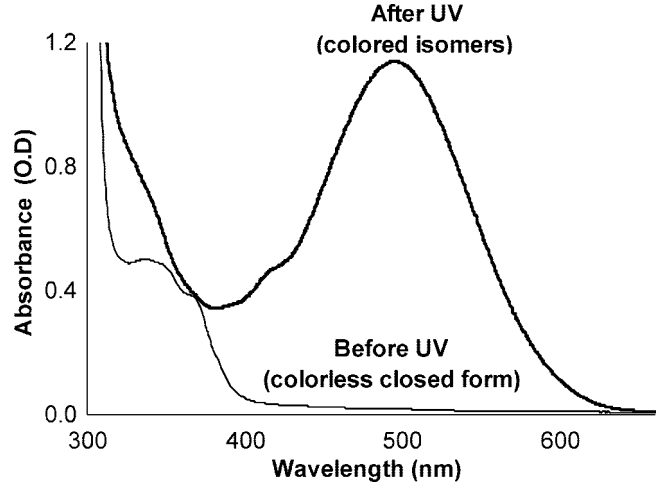

Figure 4. Absorption spectra of naphthopyran **2** in host matrix before and after 2 min of UV irradiation.

Table 2. Photokinetic Analysis of the Decoloration of Poly(2-ethylhexyl acrylate)-naphthopyran Conjugates Relative to the Control Naphthopyran 2 in Host Matrix (PEGMA/EBPDMA 1:4 Mass Composition)[a]

sample	λ_{max} (nm)[b]	M_n[c]	A_0[d]	k_1 (min^{-1})	A_1	k_2 (min^{-1})	A_2	A_{th}	$t_{1/2}$ (s)[e]
2 (toluene)[f]	483		1.22	0.91	0.72	0	0	0.23	63
2	500		0.96	0.59	0.55	0.07	0.16	0.27	173
6a	496	1,900	1.25	0.82	0.66	0.13	0.08	0.24	89
6b	492	6,300	1.10	0.90	0.73	0.07	0.03	0.22	70
6c[g]	477	11,700	0.58	0.86	0.71	0	0	0.26	73
11	484	10,400	0.95	0.94	0.74	0.03	0.03	0.21	64

[a] Samples initially irradiated at 350−400 nm for 1000 s, then thermal decoloration monitored at λ_{max} of the colored form (predetermined by wavelength scan of colored form). [b] At 20 °C in the dark for 4800 s. [c] Molecular weight (M_n, g/mol) of purified conjugates estimated from GPC analysis: poly(2-ethylhexyl acrylate) equivalents obtained using Mark-Howink parameters on a PS calibration. [d] Measured absorbance intensity at onset of thermal decoloration period. [e] Time taken for the initial absorbance value, A_0, to decay to half of its original value. [f] 10^{-5} M in toluene, fitted to $A(t) = A_1e^{-kt} + A_{th}$. [g] Conjugate doped at half concentration (0.75×10^{-7} mol/g due to mild phase separation of conjugate in the host).

Table 3. Photokinetic Analysis of the Decoloration of High T_g Methacrylate−Naphthopyran Conjugates Relative to the Control 2 in Host Matrix (PEGMA/BPDMA 1:4 Mass Composition)[a]

sample	M_n[b]	A_0[c]	k_1 (min^{-1})	A_1	k_2 (min^{-1})	A_2	A_{th}	$t_{1/2}$ (s)[d]	T_g[e]
2		1.22	0.59	0.61	0.07	0.12	0.25	144	
7a	5200	1.26	0.67	0.68	0.11	0.09	0.22	106	102.8
7b	12 300	1.10	0.64	0.66	0.10	0.10	0.22	116	117.8
7c	16 900	0.97	0.60	0.66	0.10	0.11	0.21	120	121.4
7d	18 400	1.07	0.58	0.64	0.09	0.13	0.22	135	121.6
7e	19 100	1.07	0.54	0.61	0.08	0.14	0.23	151	122.0
7f	24 000	0.98	0.49	0.58	0.07	0.16	0.23	180	122.0
9	12 500	1.11	0.50	0.55	0.06	0.21	0.22	189	127.1
2		0.90	0.61	0.61	0.07	0.11	0.25	137	
8a	3900	0.63	0.52	0.56	0.07	0.18	0.23	177	134.4
8b	4300	0.49	0.48	0.54	0.07	0.20	0.23	198	135.7
8c	5400	0.52	0.47	0.52	0.06	0.21	0.23	219	140.4
8d	10 600	0.37	0.45	0.49	0.06	0.23	0.24	252	145.0
8e	12 100	0.33	0.45	0.48	0.06	0.24	0.25	273	145.2
10	9 500	0.51	0.43	0.47	0.05	0.28	0.24	342	144.8

[a] Samples initially irradiated at 350−400 nm for 1000 s, then decoloration monitored at λ_{max} of the colored form (500 nm for all, predetermined by wavelength scan of colored form) at 20 °C in the dark for 4800 s. [b] Molecular weight (M_n, g/mol) estimated from GPC analysis: calibration with pMMA standards was used for M_n evaluation of pMMA conjugates and PS calibration used for pCEM conjugates. [c] Measured absorbance intensity at onset of thermal decoloration period. [d] Time taken for the initial absorbance value, A_0, to decay to half of its original value. [e] Thermal analysis of conjugates evaluated using a Mettler Toledo DSC 821 apparatus.

values were required to induce the same increases in kinetics with respect to their controls. This is to be expected from longer aliphatic and branched side chains providing a stronger lubricating effect. An inspection of the fitted kinetic data (Table 2) also reveals a diminishing contribution from the slower kinetic component, k_2, for the conjugates so that **6c** could be fitted to the first-order kinetics that is displayed by **2** in solution.

The pEHA conjugates also displayed increasingly significant hypsochromic shifts in their absorption spectra (as much as 23 nm for sample **6c** and 16 nm for copolymer **11**) compared to control **2** in the host matrix. Naphthopyrans have a weakly polar ground state that approaches the configuration of a quinoidal form, and the transition to their first excited state results in an increase in the dipole moment. Therefore, an increase in the medium polarity can result in the stabilization of the excited state relative to the ground state with absorption bands shifted accordingly.[53,54] The hypsochromic shifts that were seen for **11** and **6b** (484 and 492 nm) can be ascribed to the napthopyran moieties being effectively insulated from the more polar matrix environment (which comprises substantial PEG units) as a result of conjugation to pEHA. This is particularly evident for **11**, which displays the largest shift.

These factors (both kinetic enhancements and shifts in wavelength of colored form) all suggest a pronounced level of encapsulation offered by pEHA conjugation. Nonetheless, the limited M_n range for the end-functionalized conjugates that could be incorporated within the matrix meant that the kinetic enhancement and tuning ability offered by this polymer system could not be further explored.

The capacity for the methacrylate polymers (pMMA and pCEM) to add rigidity to local domains was first confirmed by their high T_g values (Table 3); the bulky carbazole side groups

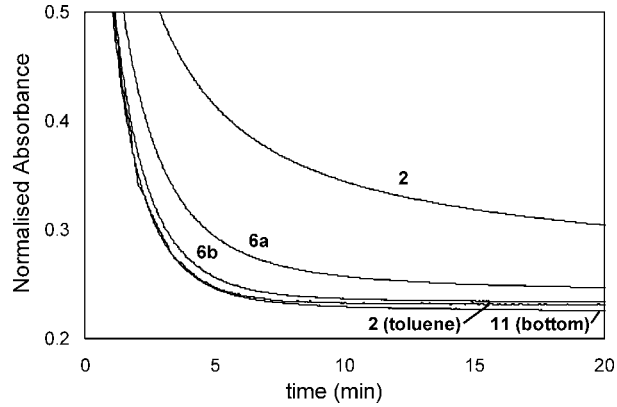

Figure 5. Normalized thermal decoloration curves (monitored in the dark at 20 °C after UV irradiation for 1000 s) of poly(2-(ethylhexyl acrylate) naphthopyran conjugates **11**, **6b**, **6a**, and control **2** in host matrix compared with the control **2** in toluene.

of pCEM conjugates were able to impart further stiffness and rigidity to local domains, beyond that of pMMA.[55] Given that the testing temperature (20 °C) was far below their T_g values, this would entail a significant restriction to movement within entangled chains. Analogous to previous research using this technique to investigate a series of end-functionalized spirooxazine high-T_g polymer conjugates (namely pMMA and *p*-styrene), the rates of thermal decay were found to slow directly with increasing molecular weight and chain length of the attached tail.[36,37] A similar pattern was observed with these results (**7a**−**f** and **8a**−**e**) also indicative of increasing encapsulation. Chain length plays the dominant role in generating increasingly restrictive domains for the photochromic transitions

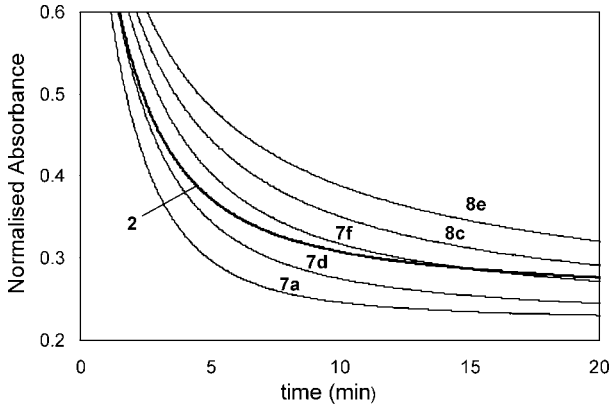

Figure 6. Thermal decoloration curves (monitored in the dark at 20 °C after UV irradiation for 1000 s) of various methacrylate naphthopyran end-functionalized conjugates and control **2** in host matrix.

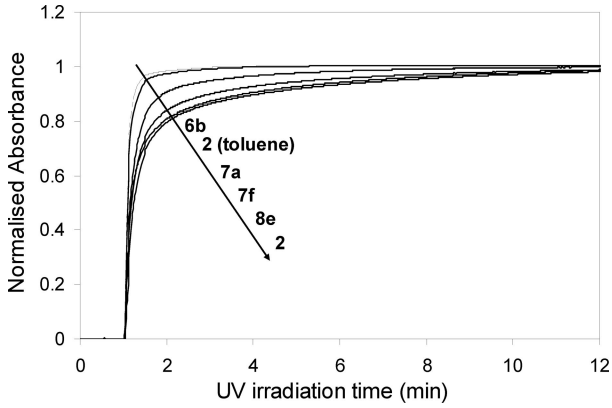

Figure 7. Normalized coloration of various end-functionalized conjugates and control **2** in PEGDMA/EBPDMA host matrix relative to control **2** in toluene; listed from fastest (**6b**) to slowest (**2**).

resulting in systematically increasing $t_{1/2}$ values and decreasing rates of decoloration for both polymer types. What is also evident from normalized decoloration curves (Figure 6) is that for this already slow photochromic dye, high-T_g tailing did not universally produce slower kinetics compared to control **2** in the host matrix; in fact, this was only established at a pronounced molecular weight of pMMA ($M_n \approx 18\,000$ g/mol).

It appears that the ability to depress the photochromic transitions (both coloration and decoloration) by using increasingly longer and rigid tailing also remains universally applicable for naphthopyrans: kinetic responses were depressed fourfold across the end-functionalized conjugates tested ($t_{1/2}$ values ranging from 70 to 273 s). However, we have now found that the onset M_n at which this effect takes place ultimately depends on the dye. The overall speed of the dye conjugate within the host is complex and is therefore determined by many interplaying factors: the thermodynamics of the dye itself, governed by electronic substitution and steric constraints, as well as subsequent effects, such as the overall rigidity of the local environment.

Concurrent Influence of Local Rigidity: Colorability Evaluation. The initial photocoloration period is marked by competitive thermal and photochemical pathways interconverting the isomers, and this results in very complex overall kinetics.[56] However, a comparison of normalized coloration curves can be insightful enough to distinguish general trends, as displayed in Figure 7, which shows a general retardation trend in the overall rate of attainment of the photosteady state with increasing rigidity of the attached polymer. The most striking effect is shown by the difference in the overall speed of the

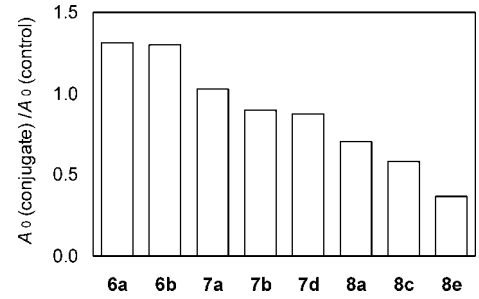

Figure 8. Measured absorbance intensity, A_0, at the onset of the thermal decoloration period of various naphthopyran end-functionalized conjugates (**6a**, **6b**, **7a**, **7b**, **7d**, **8a**, **8c**, **8d**) with respect to the control **2** in the host matrix PEGDMA/EBPDMA (1:4) with dye concentration 1.50×10^{-7} mol/g.

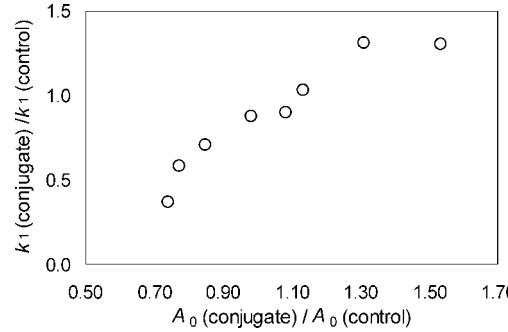

Figure 9. Evolution of k_1(conjugate)/k_1(control) with A_0(conjugate)/A_0(control) of naphthopyran end-functionalized conjugates (**6a**, **6b**, **7a**, **7b**, **7d**, **8a**, **8c**, **8d**) in the host matrix PEGDMA/EBPDMA (1:4) with dye concentration 1.50×10^{-7} mol/g.

control **2** between solution and the host matrix and the beneficial role that pEHA conjugation can play in reinstating fast coloration speed to the dye in the matrix.

Studies on photochromic coloration behavior in solution[57] have shown that the maximum intensity of color (colorability/optical density, A_0) that is achievable by a photochromic can be influenced by changes in the thermal reverse processes because these can affect the amount of colorless form that is able to convert photochemically during the steady-state irradiation. Given that our methodology has a significant influence on the thermal decoloration process, a survey of the colorability of the samples was warranted. This was carried out by comparing the A_0 value of the samples achieved by the end of the UV irradiation period with respect to the control sample **2**, which contained the same concentration of photochromic moiety and was prepared and tested with the corresponding conjugates (i.e., under the same testing conditions). Interestingly, as seen in Figure 8, a general reduction in colorability was found to occur with conjugates of increasing T_g (values listed in Tables 2 and 3). Furthermore, a notable decrease in the major thermal bleaching constant, k_1, with respect to that of the control **2** was also found to be associated with this overall decrease in colorability (Figure 9). Enhanced colorability has also been separately displayed for this dye when conjugated to lubricating poly(dimethylsiloxane) and poly(ethyleneglycol) tails (the subject of a separate publication) and has been manifested for a similar naphthopyran conjugated to a low-T_g polymer (*n*-butyl acrylate).[40]

There is the potential for coloration to be diminished in a rigid environment because the photochromic molecules can experience increasing difficulty in achieving the necessary conformations for ring opening and isomerization. Both the rate of ring opening and the frequency of necessary configurations leading to the correct activated state can be compromised.

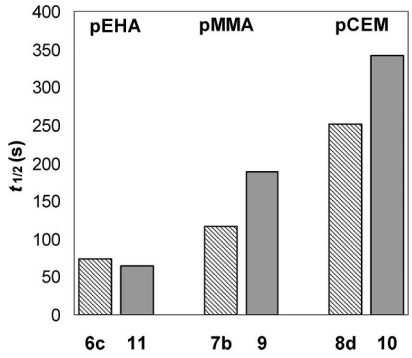

Figure 10. Thermal decoloration behavior of the colored form of naphthopyran conjugates (monitored in the dark at 20 °C after UV irradiation for 1000 s): pEHA: poly(2-ethylhexyl acrylate); pMMA: poly(methyl methacrylate); pCEM: poly(carbazolylethyl methacrylate); $t_{1/2}$ of naphthopyran end-functionalized conjugates (**6b**, **7d**, and **8d**) versus corresponding M_n naphthopyran copolymers (**11**, **9**, and **10**) in the host matrix PEGDMA/EBPDMA (1:4). Dye concentration: 1.5×10^{-7} mol/g (**7b** and **8d**), 0.75×10^{-7} mol/g (**6b**, **11**, and **9**), and 1.0×10^{-7} mol/g (**8d**).

Whether these effects are general and common to other classes of photochromics is still under investigation.

Copolymerized Naphthopyran Monomers versus End-Functionalized Conjugates. The location of the naphthopyran moiety in the final polymer chain is a factor that can affect the capacity of polymer conjugation to regulate the photochromic kinetics. As previously mentioned, the end-functionalized conjugates have the naphthopyran positioned precisely at the end of each polymer chain. This approach has been greatly exploited in our laboratories because it has the benefit of controlling the exact location of the dye moiety with respect to the polymer backbone as well as the final quantity. Furthermore, it has allowed us to discriminate interplaying factors that influence the kinetics within a host matrix such as the nature and length of the chain, the level of encapsulation, and the subsequent local rigidity. When the naphthopyran is utilized as a monomer during the polymerization process, the final conjugate will consist of statistically distributed dye units pendant from the backbone. Logically, the conjugates can be synthesized to contain more than one naphthopyran unit per chain. This effectively lowers the doping concentration of the conjugate which is needed to attain comparable levels of coloration within the host matrix. Nonetheless, compared with the end-functionalized approach, one is not able to regulate the exact location of the dye; furthermore, there is no guarantee that the polymerization will completely convert all photochromic monomer units to polymer chains. Whereas we have not fully explored the capacity of such an approach to tune kinetics within the host matrix, recent advances have shown that Y-branching architecture, which places the dye in the middle of the chain, may be the best compromise for a precise yet in-chain placement.[40]

A greater interaction of pendant naphthopyran moieties with other monomer units within the copolymer is expected, making the photochromic monomer system less dependent on chain coiling and encapsulation in order to manifest a kinetic response. The naphthopyran copolymers hence displayed a pronounced effect on kinetics as a result changes to local rigidity. As can be seen in Figure 10, a comparison of the $t_{1/2}$ values for thermal decoloration showed that each naphthopyran copolymer sample displayed a stronger effect on kinetics compared with the end-functionalized naphthopyran samples of comparable M_n values. (In Tables 2 and 3, compare **6c** vs **11**, **7b** vs **9**, and **8d** vs **10**.) First, in a low T_g environment, the pEHA−naphthopyran copolymer **11** was faster (lower $t_{1/2}$) compared with the end-functionalized comparison **6c**, and both of the pMMA and pCEM copolymer samples, **9** and **10**, were much slower (higher $t_{1/2}$) compared with similar molecular weight end-functionalized conjugates, **7b**and **8d**, respectively.

These results are preliminary; however, they exemplify that both dye-functionalized radical initiators and monomers can be exploited with controlled polymerization techniques to synthesize dye−polymer conjugates. Above all, both are practical strategies with beneficial aspects worth considering for controlling photochromic performance.

Conclusions

This Article showed that polymer conjugation can be applied to naphthopyran dyes to comprehensively regulate their switching speed within a rigid host environment. By carrying out a survey on a range of conjugates of various polymer types synthesized by ATRP, broad tuning of the photochromic decoloration kinetics was achieved by modulation of local rigidity. Systematic tuning was displayed by modifying the chain length of end-functionalized conjugates made from a naphthopyran-functionalized ATRP initiator. A comparison of their kinetics to an unconjugated control indicated that the M_n necessary to induce a slowing effect within the host matrix depends on the dye, as exemplified by the pMMA example. Enhanced coloration was found to be a concurrent effect to an increase in speed, a trend that we will continue to monitor for other photochromic classes. Naphthopyran copolymer comparisons made from functionalized monomers displayed pronounced photochromic responses demonstrating a stronger influence of conjugated polymer tails on pendant naphthopyran moieties. The comprehensive examination confirmed that polymer conjugation using ATRP is a practical strategy for methodically altering the kinetics of naphthopyrans within a broad range and a competitive alternative to modifying the electronic structure of the dye or their host matrix.

Experimental Details

Materials. All chemicals (reagents and solvents) were of high purity and were used as received unless otherwise stated. Methyl methacrylate (99% Aldrich) was purified by passing through aluminum oxide 90 (activated basic, 0.063 to 0.200 nm, Merck) to remove inhibitors. *N*-(*n*-Pentyl)-2-pyridylmethanimine was synthesized as described in literature.[58] 1-(4-Methoxy-phenyl)-1-phenyl-prop-2-yn-1-ol was synthesized from 4-methoxybenzophenone from a procedure described in literature.[13] Methyl-1,4-dihydroxynaphthalene-2-carboxylate was directly synthesized from 1,4-dihydroxy-2-naphthoic acid using methyl iodide.[59]

All reagents were purchased from Aldrich Chemical unless otherwise stated. All chromatography was performed using silica gel (Kieselgel Merck 60, 0.040 to 0.063 mm), and TLC was performed on Merck Silica $60F_{254}$ plates.

General Experimental Measurements. Gel permeation chromatography (GPC) was performed on a Waters 515 HPLC pump and Waters 717 plus autosampler equipped with Waters 2414 refractive index detector and three mixed-C PLgel columns (7.5×300 mm^2, 5 μm particle size, linear molecular weight range 200−2 000 000) and one mixed-E PLgel column (7.5×300 mm^2, 3 μm particle size, linear molecular weight range up to 30 000) from Polymer Laboratories. Tetrahydrofuran (THF) with a flow rate of 1.0 mL/min was used as eluent at 22 ± 2 °C. Molecular weights for poly(2-(*N*-carbazolyl)ethyl methacrylate) conjugates were calculated via calibration with narrow polydispersity polystyrene standards (Polymer Laboratories) ranging from 600 to 7.5×10^6 g/mol. Molecular weights (M_n) of poly(2-ethylhexyl acrylate) conjugates were calculated using Mark-Howink parameters[60] on the PS calibration. The system was also calibrated with narrow poly(methyl methacrylate) standards in the range of 500 to 10^6 g/mol to derive M_n values of pMMA conjugates. Number (M_n) and

weight-average (M_w) molecular weights were evaluated using Waters Millennium/Empower software. A third-order polynomial was used to fit the log M versus time calibration curve, which appeared to be linear across the molecular weight ranges.

^{1}H (400 MHz) and ^{13}C NMR (100 MHz) spectra were obtained with a Bruker Av400 spectrometer at 25 °C. Spectra were recorded for samples dissolved in deuterated solvent, and chemical shifts are reported as parts per million from external tetramethylsilane. Monomer conversions were obtained from the ^{1}H NMR spectra. The resonances integrated to obtain conversions for EHA polymerizations were the vinyl peaks at 5.8 and 6.4 ppm (monomer only) and the OCH_2- peaks at 3.9 to 4.1 ppm (monomer and polymer). The resonances integrated to obtain conversions for MMA polymerizations were the vinyl peaks at 5.6 and 6.1 ppm (monomer only) and the OCH_3 peaks at 3.6 to 3.7 ppm (monomer and polymer). For CEM polymerizations, the integrated resonances were the vinyl peaks at 5.8 and 5.9 ppm (monomer) and the aromatic carbazole region (Ar−H, 2H) between 7.8 and 8.2 ppm (monomer and polymer). The compositional ratio of the copolymers was calculated by ^{1}H NMR via the integrated peak intensity ratio of naphthopyran versus polymer. All other spectra were recorded on a Bruker Av400 spectrometer.

2D NMR standard gradient DQF-COSY, HSQC, and HMBC experiments were acquired for resonance assignment purposes of naphthopyran derivatives **1**−**5**.

Positive ion EI mass spectra were run on a ThermoQuest MAT95XL mass spectrometer using ionization energy of 70 eV. Accurate mass measurements were obtained with a resolution of 5000−10 000 using PFK as the reference compound.

Thermal analysis by differential scanning calorimetry (DSC) was performed to determine the T_g of the conjugates. This was carried out using a Mettler Toledo DSC821 machine with temperature and heat flow calibrated using indium and zinc as reference substances. Samples (∼10 mg) were heated under nitrogen from 0 to 160 °C at 10 °C/min to remove the thermal history and then from 0 to 200 °C at 10 °C/min. The T_g values were taken from the midpoints of the heat flow changes from the second heat cycle.

Photochromic Analysis. Under UV−vis continuous irradiation, the photochromic responses of the samples were analyzed on a light table composed of a Cary 50 spectrophotometer to measure the absorbance and a 160 W Oriel xenon lamp as an incident light source. A series of two filters (Edmund Optics 320 cutoff and bandpass filter U-340) were used to restrict the output of the lamp to a narrow band (350−400 nm). The samples were maintained at 20 °C and monitored at their maximum absorbance of the colored form (normally 500 nm unless otherwise stated) for a period of 1000 s. Then, the thermal decoloration was monitored in the absence of UV irradiation for an additional 6000 s. The solution comparison was carried out with sample **2** in toluene (10^{-5} M) in a quartz cell of 1 cm path length.

Synthesis Procedures. *Methyl 6-Hydroxy-2-(4-methoxyphenyl)-2-phenyl-2H-naphtho[1,2-b]pyran-5-carboxylate (**4**).*[46] A mixture of 1-(4-methoxy-phenyl)-1-phenylprop-2-yn-1-ol (3.3 g, 13.7 mmol), methyl 1,4-dihydroxynapthalene-2-carboxylate (3.0 g, 13.7 mmol), *p*-toluenesulfonic acid monohydrate (0.24 g, 1.38 mmol), and silica gel 60 (5.8 g) was ground for 10 min at room temperature using a mortar and pestle, and the mixture was then left to stand for 1 h. The reaction mixture was then passed through a short silica filtration column with toluene to remove a large portion of darkened baseline material. The bright orange filtrate was concentrated in vacuo to give a gummy orange material that was then purified by column chromatography on silica gel using toluene as the eluent. The solvent was evaporated in vacuo, and the resulting orange oil was treated with a small amount of diethyl ether/hexane. The product crystallized from solution, giving a bright yellow solid. (4.3 g, 71% yield). ^{1}H NMR (400 MHz, d_6-acetone, δ): 3.72 (s, 3H, OCH_3), 4.04 (s, 3H, $COOCH_3$), 6.37 (d, J 9.88 Hz, 1H, H-3), 6.84 (apparent d, J = 8.78 Hz, 2H, H-3″), 7.22−7.25 (m, 1H, H-4′), 7.31−7.34 (m, 2H, H-3′), 7.47 (apparent doublet, J = 8.78 Hz, 2H, H-2″), 7.51 (d, J = 9.88 Hz, 1H, H-4), 7.56−7.61 (m, 3H, H-2′ and H-9), 7.73−7.77 (m, 1H, H-8), 8.32 (d, J = 8.42 Hz, 1H, H-10), 8.42 (d, J = 8.42 Hz, 1H, H-7), 12.19 (s, 1H, OH). ^{13}C NMR (100 MHz, d_6-acetone, δ): 53.14 ($COO\underline{C}H_3$), 55.54 (OCH_3), 81.98 (C-2), 103.25 (C-5), 114.33 (C-3″), 114.60 (C-4a), 122.83 (C-7), 124.53 (C-4), 124.80 (C-10), 126.02 (C-10a), 127.33 (C-2′), 127.67 (C-9), 128.22 (C-4′), 128.83 (C-3), 128.92 (C-2″), 129.01 (C-3′), 129.52 (C-6a), 130.87 (C-8), 137.61 (C-2a), 141.94 (C-1a), 146.22 (C-2b), 157.22 (C-6), 160.10 (C-4″), 173.00 ($\underline{C}OOCH_3$). Refer to Figure 11 for the corresponding (nonstandard) numbering system used for NMR assignments of compound **1**. MS (EI) *m*/*z*: 438.1 ([M]$^+$ 28%), 405.1 (19), 375.1 (16), 361.1 (13), 298.0 (12), 289.1 (14), 276.1 (12), 203.1 (13). MS (HR, EI) *m*/*z*: 438.1456 ($C_{28}H_{22}O_5$ requires 438.1462).

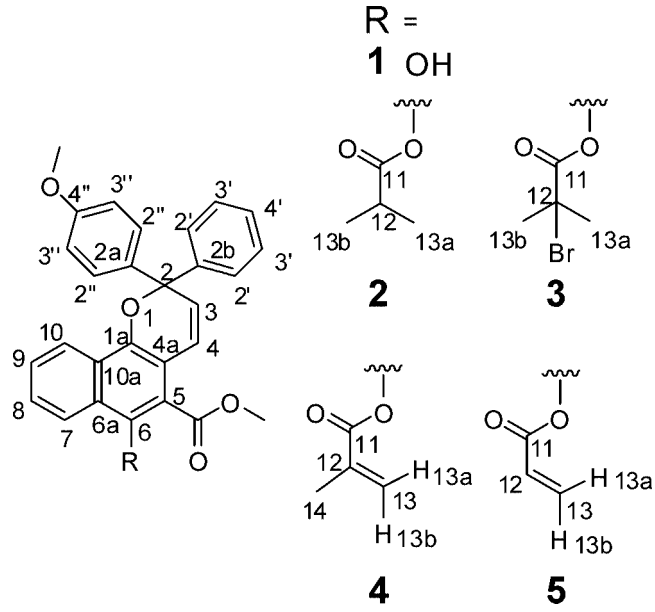

Figure 11. Nonstandard numbering system used for compounds **1**−**5**.

*Methyl 6-(Isobutyryloxy)-2-(4-methoxy-phenyl)-2-phenyl-2H-naphtho[1,2-b]pyran-5-carboxylate (**2**).* To an ice-cooled solution of methyl 6-hydroxy-2-(4-methoxyphenyl)-2-phenyl-2*H*-naphtho[1,2-*b*]pyran-5-carboxylate, were added **1** (0.18 g, 0.41 mmol) and triethylamine (TEA) (0.14 mL, 1.0 mmol) in dry dichloromethane (CH_2Cl_2) (7 mL) dropwise and isobutyryl chloride (0.09 mL, 0.86 mmol) under argon. The solution was stirred with cooling for 0.5 h and was then left to be stirred for an additional 12 h at room temperature. The solvent was evaporated in vacuo, and the residue was redissolved in diethyl ether (Et_2O) (30 mL) and washed successively with 0.5 M HCl, water, aqueous $NaHCO_3$, water, and brine. The organic layer was dried with $MgSO_4$, and the solvent was evaporated in vacuo. The crude product was purified by column chromatography (silica gel 60, CH_2Cl_2), giving the product as pale tan-colored crystals (160 mg, 77%). ^{1}H NMR (400 MHz, d_6-acetone, δ): 1.35 (d, J = 6.95 Hz, 6H, H-13a and H-13b), 2.90 (sept, J = 6.95 Hz, 1H, H-12), 3.73 (s, 3H, OCH_3), 3.91 (s, 3H, $COOCH_3$), 6.46 (d, J = 9.88 Hz, 1H, H-3), 6.87 (apparent d, J = 8.78 Hz, 2H, H-3″), 6.96 (d, J = 9.88 Hz, 1H, H-4), 7.24−7.28 (m, 1H, H-4′), 7.33−7.37 (m, 2H, H-3′), 7.46 (apparent doublet, J = 8.78 Hz, 2H, H-2″), 7.55−7.62 (m, 3H, H-2′ and H-9), 7.65−7.69 (m, 1H, H-8), 7.80 (d, J = 8.42 Hz, 1H, H-10), 8.44 (d, J = 8.42 Hz, 1H, H-7). ^{13}C NMR (100 MHz, d_6-acetone, δ): 19.35 (C-13a and 13b), 34.74 (C-12), 52.95 ($COO\underline{C}H_3$), 55.56 (OCH_3), 83.67 (C-2), 114.30 (C-4a), 114.46 (C-3″), 121.17 (C-5), 121.86 (C-4), 123.12 (C-7), 123.31 (C-10), 127.05 (C-6a), 127.42 (C-2′), 128.32 (C-10a), 128.47 (C-4′), 128.78 (C-9), 128.85 (C-8), 129.03 (C-2″), 129.16 (C-3′), 130.14 (C-3), 137.44 (C-2a), 140.09 (C-6), 145.98 (C-2b), 146.71 (C-1a), 160.28 (C-4″), 166.38 ($\underline{C}OOCH_3$), 175.46 (C-11). Refer to Figure 11 for the corresponding (nonstandard) numbering system used for NMR assignments of compound **2**. MS (EI) *m*/*z*: 508.2 ([M]$^+$ 28%), 437.1 (18), 405.1 (31), 377.1 (31),

361.1 (10). MS (HR, EI) *m/z*: 508.1881 ($C_{32}H_{28}O_6$ requires 508.1880).

*Methyl 6-(2-Bromo-2-methylpropanoyloxy)-2-(4-methoxy-phenyl)-2-phenyl-2H-naphtho[1,2-b]pyran-5-carboxylate (**3**).* This compound was synthesized from **1** and 2-bromo-isobutyrylbromide using the same general procedure as that above and was isolated as a peach-colored glassy solid (520 mg, 78%) after purification by column chromatography (silica gel 60, CH_2Cl_2) and recrystallization from diethyl ether. ^{1}H NMR (400 MHz, d_6-acetone, δ): 2.13 (6H, s, H-13a and H-13b), 3.74 (s, 3H, OCH_3), 3.94 (s, 3H, $COOCH_3$), 6.48 (d, $J = 9.88$ Hz, 1H, H-3), 6.88 (apparent d, $J = 8.78$ Hz, 2H, H-3″), 6.97 (d, $J = 9.88$ Hz, 1H, H-4), 7.25−7.29 (m, 1H, H-4′), 7.34−7.38 (m, 2H, H-3′), 7.46 (apparent d, $J = 8.78$ Hz, 2H, H-2″), 7.55−7.57 (m, 2H, H-2′), 7.65−7.70 (m, 2H, H-8, H-9), 8.02 (d, $J = 8.42$ Hz, 1H, H-10), 8.47 (d, $J = 8.42$ Hz, 1H, H-7). ^{13}C NMR (100 MHz, d_6-acetone, δ): 31.21 (C-12), 53.26 ($COO\underline{C}H_3$), 55.60 (OCH_3), 56.65 (C-12), 83.80 (C-2), 114.31 (C-3″), 114.48 (C-4a), 121.08 (C-5), 121.78 (C-4), 122.97 (C-10), 123.24 (C-7), 127.12 (C-6a), 127.42 (C-2′), 128.08 (C-10a), 128.52 (C-4′), 129.05 (C-9), 129.08 (C-8), 129.10 (C-2″), 129.20 (C-3′), 130.32 (C-3), 137.33(C-2a), 139.47 (C-6), 145.87(C-2b), 147.20 (C-1a), 160.31 (C-4″), 166.15 ($\underline{C}OOCH_3$), 170.48 (C-11). Refer to Figure 11 for corresponding (nonstandard) numbering system used for NMR assignments of compound **3**. MS (EI) *m/z*: 586.1 ($[M]^+$ 17%), 506 (10), 475.1 (20), 437.1 (29), 405 (100), 377.1 (63), 289.1 (15), 121.0 (11), 69.1(11). MS (HR, EI) *m/z*: 586.0987 ($C_{32}H_{27}BrO_6$ requires 586.0986).

*Methyl 6-(Methacryloyl)-2-(4-methoxy-phenyl)-2-phenyl-2H-naphtho[1,2-b]pyran-5-carboxylate (**4**).* This compound was synthesized from **1** and methacryloyl chloride using the same general procedure as that above and was isolated as a cream-colored solid after purification by column chromatography (silica gel 60, 1:1 Et_2O/Hexane) (480 mg, 86%). ^{1}H NMR (400 MHz, d_6-acetone, δ): 2.09 (s, 3H, H-14), 3.73 (s, 3H, OCH_3), 3.86 (s, 3H, $COOCH_3$), 5.91−5.92 (m, 1H, H-13a), 6.39 (broad s, 1H, H-13b), 6.46 (d, $J = 9.88$ Hz, 1H, H-3), 6.88 (apparent d, $J = 8.78$ Hz, 2H, H-3″), 7.01 (d, $J = 9.88$ Hz, 1H, H-4), 7.25−7.28 (m, 1H, H-4′), 7.34−7.37 (m, 2H, H-3′), 7.47 (apparent d, $J = 8.78$ Hz, 2H, H-2″), 7.56−7.62 (m, 3H, H-2′ and H-9), 7.66−7.70 (m, 1H, H-8), 7.81 (d, $J = 8.42$ Hz, 1H, H-10), 8.46 (d, $J = 8.42$ Hz, 1H, H-7). ^{13}C NMR (100 MHz, d_6-acetone, δ): 18.58 (C-14), 52.86 ($COO\underline{C}H_3$), 55.57 (OCH_3), 83.67 (C-2), 114.19 (C-4a), 114.46 (C-3″), 120.90 (C-5), 121.89 (C-4), 123.12 (C-7), 123.50 (C-10), 127.14 (C-6a), 127.42 (C-2′), 128.17 (C-13), 128.34 (C-10a), 128.47 (C-4′), 128.82 (C-9), 128.98 (C-8), 129.04 (C-2″), 129.17 (C-3′), 130.18 (C-3), 136.51 (C-12), 137.42 (C-2a), 140.55 (C-6), 145.96 (C-2b), 146.84 (C-1a), 160.28 (C-4″), 166.11 (C-11), 166.25 ($\underline{C}OOCH_3$). Refer to Figure 11 for corresponding (nonstandard) numbering system used for NMR assignments of compound **4**. MS (EI) *m/z*: 506.2 ($[M]^+$ 33%), 474.1 (11), 437.1 (38), 405.1 (100), 377.1 (54), 69.2 (13). MS (HR, EI) *m/z*: 506.1723 ($C_{32}H_{26}O_6$ requires 506.1724).

*Methyl 6-(Acryloyl)-2-(4-methoxy-phenyl)-2-phenyl-2H-naphtho-[1,2-b]pyran-5-carboxylate (**5**).* This compound was synthesized from **1** and acryloyl chloride using the same general procedure as that above and was isolated as a cream-colored solid after purification by column chromatography (silica gel 60, 1:1 Et_2O/Hexane) (250 mg, 86%). ^{1}H NMR (400 MHz, d_6-acetone, δ): 3.73 (s, 3H, OCH_3), 3.86 (s, 3H, $COOCH_3$), 6.18 (dd, $J = 10.24$ Hz, $J = 1.46$ Hz, 1H, H-13b), 6.46 (d, $J = 9.88$ Hz, 1H, H-3), 6.51 (d, $J = 10.24$ Hz, 1H, H-12), 6.63 (dd, $J = 17.20$ Hz, $J = 1.46$ Hz, 1H, H-13a), 6.88 (apparent d, $J = 8.78$ Hz, 2H, H-3″), 7.01 (d, $J = 9.88$ Hz, 1H, H-4), 7.25−7.28 (m, 1H, H-4′), 7.34−7.37 (m, 2H, H-3′), 7.47 (apparent doublet, $J = 8.78$ Hz, 2H, H-2″), 7.56−7.62 (m, 3H, H-2′ and H-9), 7.66−7.70 (m, 1H, H-8), 7.81 (d, $J = 8.42$ Hz, 1H, H-10), 8.46 (d, $J = 8.42$ Hz, 1H, H-7). ^{13}C NMR (100 MHz, d_6-acetone, δ): 52.90 ($COO\underline{C}H_3$), 55.57 (OCH_3), 83.70 (C-2), 114.44 (C-4a), 114.48 (C-3″), 120.99 (C-5), 121.85 (C-4), 123.15 (C-7), 123.45 (C-10), 127.13 (C-6a), 127.43 (C-2′), 128.25 (C-12), 128.31 (C-10a), 128.49 (C-4′), 128.87 (C-9), 129.01 (C-8), 129.05 (C-2″), 129.18 (C-3′), 130.20 (C-3), 133.90 (C-13), 137.45 (C-2a), 140.18 (C-6), 145.996 (C-2b), 146.91 (C-1a), 160.31 (C-4″), 164.87 (C-11), 166.22 ($\underline{C}OOCH_3$). Refer to Figure 11 for the corresponding (nonstandard) numbering system used for NMR assignments of compound **5**. MS (EI) *m/z*: 492.1 ($[M]^+$ 34%), 460.1 (15), 437.1 (30), 405.1 (100), 377.1 (71), 334.1 (12), 318.1 (10), 305.1 (10), 289 (13), 55 (12). MS (HR, EI) *m/z*: 492.1569 ($C_{31}H_{24}O_6$ requires 492.1573).

2-(9H-Carbazol-9-yl) Ethyl Methacrylate (CEM). A solution of methacryloyl chloride (distilled, 3.50 mL, 35.6 mmol) was slowly added via a gastight syringe to a solution of triethylamine (4.95 mL, 35.6 mmol) and 2-(9*H*-carbazol-9-yl)ethanol (5 g, 23.7 mmol) in dry THF (200 mL). The mixture was kept under an inert atmosphere of argon and cooled to 0 °C during the addition and was then left to be stirred for an additional 12 h at room temperature. The solvent was evaporated in vacuo and then redissolved in CH_2Cl_2 (150 mL) and washed successively with water (2 × 100 mL) and saturated brine. The organic layer was dried with $MgSO_4$, and the solvent was evaporated in vacuo. The product was then purified by recrystallization with ethanol/chloroform (2:1) and isolated as a fluffy white solid (3.4 g, 52%). ^{1}H NMR (400 MHz, $CDCl_3$, δ): 1.81 (s, 3H, CH_3), 4.54 (t, $J = 5.8$ Hz, 2H, CH_2), 4.63 (t, $J = 5.8$ Hz, 2H, CH_2), 5.49 (s, 1H, −C═CH), 5.94 (s, 1H, −C═CH), 7.24−7.28 (m, 2H, Ar−H), 7.44−7.48 (m, 4H, Ar−H), 8.11 (d, $J = 7.68$ Hz, Ar−H). ^{13}C NMR (100 MHz, $CDCl_3$, δ): 18.19, 41.62, 62.46, 108.59, 119.24, 120.38, 123.04, 125.76, 126.32, 135.67, 140.39, 167.26. MS (EI) *m/z*: 279.1 ($[M]^+$ 35%), 193.1 (31), 180.1 (100), 152.0 (12), 69 (14). MS (HR, EI) *m/z*: 279.1258 ($C_{18}H_{17}O_2N$ requires 279.1254).

*Atom Transfer Radical Polymerization of 2-Ethylhexylacrylate Using Naphthopyran Initiator **3**.* A 25 mL stock solution containing 2-ethylhexyl acrylate (22.10 g, 119.9 × 10^{-3} mol, 4 M), naphthopyran initiator **3** (469.6 mg, 8 × 10^{-4} mol), and dNbpy ligand (653.4 mg, 16.0 × 10^{-4} mol) was prepared. To ampules containing CuBr (18.3 mg, 1.28 × 10^{-4} mol) were added 4 mL aliquots, and the final molar ratio of 2-EHA/**3**/ligand/CuBr was 150:1:2:1. The ampules were then degassed with three freeze−evacuate−thaw cycles, sealed, and then heated to 90 °C in a thermostatted oil bath; the polymerization was monitored for 1−7 h. End-functionalized napthopyran conjugates **6b** and **6c** were obtained from 1 and 2 h polymerization intervals, respectively. We obtained napthopyran conjugate **6a** in the same manner by preparing a 5 mL stock solution containing 2-ethylhexyl acrylate (4.42 g, 24.0 × 10^{-3} mol), naphthopyran initiator **3** (140.9 mg, 2.40 × 10^{-4} mol), and dNbpy ligand (196 mg, 4.80 × 10^{-4} mol). A 4 mL aliquot was added to an ampule containing CuBr (27.5 mg, 1.92 × 10^{-4} mol); the final molar ratio of 2-EHA/**3**/ligand/CuBr was 100:1:2:1. The ampules were then degassed with three freeze−evacuate−thaw cycles, sealed, and then heated to 90 °C in a thermostatted oil bath for 1 h. The final polymers were purified by column chromatography (silica gel 60, 1:1 CH_2Cl_2/Et_2O), followed by two separations carried out by dissolving the polymer in hexane and sequentially washing with methanol to remove the residual monomer.

*Atom Transfer Radical Polymerization of Methyl Methacrylate Using Naphthopyran Initiator **3**.* A 20 mL stock solution of methyl methacrylate (6.84 g, 6.84 × 10^{-2} mol, 3.42 M), naphthopyran initiator **3** (201 mg, 3.42 × 10^{-4} mol) and *N*-PPMA ligand (120 mg, 6.84 × 10^{-4} mol) in toluene was prepared. To ampules containing CuBr (7.4 mg, 5.13 × 10^{-5} mol) were added 3 mL aliquots; the final molar ratio of MMA/**3**/ligand/CuBr was 200:1:2:1. The ampules were then degassed with three freeze−evacuate−thaw cycles, sealed, and then heated to 90 °C in a thermostatted oil bath for 2−16 h to obtain end-functionalized napthopyran conjugates **7a−7f.** The final polymers were individually purified by two precipitations by dissolution of the crude residues in a minimal volume of CH_2Cl_2, followed by dropwise addition to excess methanol.

*Atom Transfer Radical Polymerization of CEM Using Naphthopyran Initiator **3**.* A 10 mL stock solution of 2-(9*H*-carbazol-9-yl)ethyl methacrylate (2.0 g, 7.16 × 10^{-3} mol), naphthopyran initiator **3** (42.1 mg, 7.16 × 10^{-5} mol), and *N*-PPMA ligand (25.2 mg, 1.43 × 10^{-4} mol) in toluene was prepared. To ampules containing CuBr (2.05 mg, 1.43 × 10^{-5} mol) were added 2 mL aliquots; the final

molar ratio of CEM/**3**/ligand/CuBr was 100:1:2:1. The ampules were then degassed with three freeze−evacuate−thaw cycles, sealed, and then heated to 90 °C in a thermostatted oil bath; the polymerization was monitored for 3−6 h. End-functionalized napthopyran conjugates **8a**−**8c** were obtained from 3−5 h polymerization intervals. We obtained napthopyran conjugates **8d** and **8e** by preparing a 5 mL stock solution containing 2-(9*H*-carbazol-9-yl)ethyl methacrylate (1.0 g, 3.58×10^{-3} mol), naphthopyran initiator **3** (21.0 mg, 3.58×10^{-5} mol), and PMDETA ligand (6.20 mg, 3.58×10^{-5} mol) in toluene. To two ampules containing CuBr (2.05 mg, 1.43×10^{-5} mol) were added 2 mL aliquots individually; the final molar ratio of CEM/**3**/ligand/CuBr was 100:1:1:1. The two ampules were then degassed with three freeze−evacuate−thaw cycles, sealed, and then individually heated to 90 °C in a thermostatted oil bath for 90 min and 3 h. The final polymers were individually purified by several precipitations by dissolution of the crude residues in a minimal volume of CH_2Cl_2, followed by dropwise addition to excess methanol.

Atom Transfer Radical Polymerization synthesis of p(MMA)-co-p(chromene) copolymer **9**. MMA (900 mg, 8.99×10^{-3} mol), naphthopyran methacrylate **4** (100 mg, 1.97×10^{-4} mol), ethyl-2-bromo isobutyrate initiator (8.96 mg, 4.59×10^{-5} mol), and *N*-PPMA ligand (16.2 mg, 9.18×10^{-5} mol) were dissolved in 2.6 mL of toluene. The solution was then transferred to an ampule containing CuBr (6.59 mg, 4.59×10^{-5} mol); the final molar ratio of monomers/initiator/ligand/CuBr was 200:1:2:1. The ampule was then degassed with three freeze−evacuate−thaw cycles, sealed, and then heated to 90 °C in a thermostatted oil bath for 16 h. The polymer was then purified by two precipitations by dissolution of the crude residues in a minimal volume of CH_2Cl_2, followed by dropwise addition to excess methanol.

Atom Transfer Radical Polymerization Synthesis of p(CEM)-co-p(chromene) Copolymer **10**. A 10 mL stock solution of ethyl-2-bromo isobutyrate initiator (14.40 mg, 7.38×10^{-5} mol) and PMDETA ligand (12.79 mg, 7.38×10^{-5} mol) in toluene was prepared. A 1 mL aliquot was added to CEM (194 mg, 6.95×10^{-4} mol) and naphthopyran methacrylate **4** (21.6 mg, 4.26×10^{-5} mol), and this solution was then transferred to an ampule containing CuBr (1.06 mg, 7.38×10^{-6} mol) so that the final ratio of monomers/initiator/ligand/Cu(I)Br was 100:1:1:1. The ampule was then degassed with three freeze−evacuate−thaw cycles, sealed, and then heated to 90 °C in a thermostatted oil bath for 2 h. The polymer was then purified by several precipitations by dissolution of the crude residues in a minimal volume of CH_2Cl_2, followed by dropwise addition to excess methanol.

Atom Transfer Radical Polymerization Synthesis of p(EHA)-co-p(chromene) Copolymer **11**. EHA (2.38 g, 12.9×10^{-3} mol), naphthopyran acrylate **5** (196 mg, 3.98×10^{-4} mol), ethyl-2-bromo isobutyrate initiator (26.0 mg, 1.33×10^{-4} mol), and dNbpy ligand (108 mg, 2.66×10^{-4} mol) were dissolved in 1 mL of toluene. The solution was then transferred to an ampule containing CuBr (19.10 mg, 1.3×10^{-4} mol); the final molar ratio of monomers/initiator/ligand/CuBr was 100:1:2:1. The ampule was then degassed with three freeze−evacuate−thaw cycles, sealed, and then heated to 90 °C in a thermostatted oil bath for 9.5 h. The polymer was then purified by column chromatography (silica gel 60, 1:1 CH_2Cl_2/Et_2O), followed by two separations carried out by dissolving the polymer in hexane and sequentially washing with methanol to remove the residual monomer.

Preparation of Photochromic Test Samples. Polymer photochromic conjugates were individually dissolved in a standard industrial lens formulation made up of 1:4 weight ratio of poly(ethylene glycol) (400) dimethacrylate and 2,2′-bis((4-methacryloxyethoxy)phenyl)-propane (specific monomer structures given below) with 0.4% AIBN. The samples were then cured at 80 °C for 16 h in a standard mold to give optically clear test samples of equivalent thickness (1.2 mm). End-functionalized naphthopyran conjugates (**6a**−**6c**, **7a**−**7f**, and **8a**−**8e**) and the naphthopyran control **2** were doped at equivalent concentrations of 1.5×10^{-7} mol/g of lens formulation. Copolymer conjugates **9** and **11** were doped at a concentration of 0.75×10^{-7} mol/g of lens formulation, and pCEM copolymer conjugate **10** was doped at a concentration of 1.0×10^{-7} mol/g to compensate for their higher naphthopyran contents. The final concentrations were chosen to maintain optical densities in a meaningful detector range for photochromic kinetic tests.

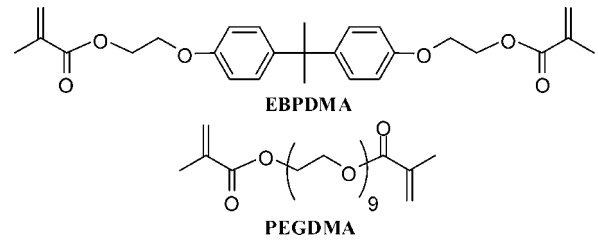

Figure 12. Structures of monomers of thermally curable host matrix formulation.

Acknowledgment. F.E. thanks the CRC for Polymers for funding the research in association with CAMD, the School of Chemical Engineering and Industrial Chemistry, and CSIRO Molecular and Health Technologies for providing laboratory space. F.E. also acknowledges the assistance of Dr. Jonathan Campbell (University of New South Wales) for the setup and maintenance of photochromic testing equipment. T.P.D. acknowledges the receipt of a Federation fellowship from the ARC.

Supporting Information Available: Example ^{1}H NMR of ATRP conjugates and initiator **3** and kinetic plots for ATRP polymerizations to give end functional conjugates. This material is available free of charge via the Internet at http://pubs.acs.org.

References and Notes

(1) Dürr, H. General Introduction. In *Photochromism: Molecules and Systems*, 1st ed.; Dürr, H., Bouas-Laurent, H., Eds.; Studies in Organic Chemistry Series 40; Elsevier: Amsterdam, 1990; Vol. 40, pp 1−14.
(2) *Organic Photochromic and Thermochromic Compounds*; Crano, J. C., Guglielmetti, R. J., Eds.; Plenum Press: New York, 1999; Vols. *1* and *2*.
(3) Kawata, S.; Kawata, Y. *Chem. Rev.* **2000**, *100*, 1777–1788.
(4) Berkovic, G.; Krongauz, V.; Weiss, V. *Chem. Rev.* **2000**, *100*, 1741–1753.
(5) Evans, R. A.; Such, G. K. *Aust. J. Chem.* **2005**, *58*, 825–830.
(6) Mendintz, I. L.; Trammell, S. A.; Mattoussi, H.; Mauro, M. *J. Am. Chem. Soc.* **2004**, *126*, 30–31.
(7) Zhu, L.; Zhu, M.-Q.; Hurst, J. K.; Li, A. D. Q. *J. Am. Chem. Soc.* **2005**, *127*, 8968–8970.
(8) Zhu, M.-Q.; Zhu, L.; Han, J. J.; Wu, W.; Hurst, J. K.; Li, A. D. Q. *J. Am. Chem. Soc.* **2006**, *128*, 4303–4309.
(9) Zhu, L.; Wu, W.; Zhu, M.-Q.; Han, J. J.; Hurst, J. K.; Li, A. D. Q. *J. Am. Chem. Soc.* **2007**, *129*, 3524–3526.
(10) Lee, H. i.; Wu, W.; Oh, J. K.; Mueller, L.; Sherwood, G.; Peteanu, L.; Kowalewski, T.; Matyjaszewski, K. *Angew. Chem., Int. Ed.* **2007**, *46*, 2453–2457.
(11) Van Gembert, B. Benzo and Naphthopyrans (Chromenes), Chapter 3. In *Organic Photochromic and Thermochromic Compounds*; Crano, J., Guglielmetti, R., Eds.; Plenum Press: New York, 1998; Vol. 1.
(12) Becker, R. S.; Michi, J. *J. Am. Chem. Soc.* **1966**, *88*, 5931–5933.
(13) Gabbutt, C. D.; Heron, M. B.; Instone, A. C.; Thomas, D. A.; Partington, S. M.; Husthouse, M. B.; Gelbrich, T. *Eur. J. Org. Chem.* **2003**, 1220–1230.
(14) Ottavi, G.; Favaro, G.; Malatesta, V. *J. Photochem. Photobiol., A* **1998**, *115*, 123–128.
(15) Delbaere, S.; Micheau, J.-C.; Vermeersch, G. *J. Org. Chem.* **2003**, *68*, 8968–8973.
(16) Delbaere, S.; Luccioni-Huoze, B.; Bochu, C.; Teral, Y.; Campredon, M.; Vermeersch, G. *J. Chem. Soc., Perkin Trans. 2.* **1998**, 1153–1157.
(17) Hobley, J.; Malatesta, V.; Hatanaka, K.; Kajimoto, S.; Williams, S.; Fukumura, H. *Phys. Chem. Chem. Phys.* **2002**, *4*, 180–184.
(18) Heron, B. M.; Gabbut, C. D.; Hepworth, J. D.; Partington, S. M.; Clarke, D. A.; Corns; S. N. Rapid Fading Photo-Responsive Materials. WO/2001/012619 A1, **2001**.
(19) Van Gemert, B. Photochromic Indeno-Fused Naphthopyran Compounds. U.S. Patent 5,645,767, **1997**.
(20) Rickwood, M.; Smith, K. E.; Gabbut, C. D.; Hepworth, J. D. Photochromic Napthopyran Compounds. U.S. Patent 5,623,005, **1997**.

(21) Momoda, J.; Komuro, Y. Chromene Compounds. U.S. Patent 6,469,076, **2002**.
(22) Manfred, M.; Herbert, Z. Diaryl-2*H*-naphthopyrans. U.S. Patent 6,036,890, **2000**.
(23) Kumar, A.; Gemert, B. V.; Knowles, D. B. Substituted Naphthopyrans. U.S. Patent 5,458,814, **1995**.
(24) Heller, H. G. Photochromic Chromene Compounds. U.S. Patent 5,200,116, **1993**.
(25) Gemert, B. V.; Bergomi, M. P. Photochromic Naphthopyran Compounds. U.S. Patent 5,066,818, **1991**.
(26) Pozzo, J.-L.; Lokshin, V.; Samat, A.; Guglielmetti, R.; Dubest, R.; Aubarb, J. *J. Photochem. Photobiol., A* **1998**, *114*, 185–191.
(27) Krongauz, V. Environmental Effects on Organic Photochromic Systems. In *Photochromism: Molecules and Systems*, 1st ed.; Dürr, H., Bouas-Laurent, H., Eds.; Studies in Organic Chemistry Series 40; Elsevier: Amsterdam, 1990; Vol. 40, p 793−820.
(28) Lyubimov, A. V.; Zaichenko, N. L.; Marevtsev, V. S. *J. Photochem. Photobiol., A* **1999**, *120*, 55–62.
(29) Ichimura, K. Photochromic Polymers. In *Organic Photochromic and Thermochromic Compounds*; Crano, J. C., Guglielmetti, R. J., Eds.; Plenum Press: New York, 1999; Vol. 2.
(30) Matyjaszewski, K.; Xia, J. *Chem. Rev.* **2001**, *101*, 2921–2990.
(31) Moad, G.; Rizzardo, E.; Thang, S. *Aust. J. Chem.* **2006**, *59*, 669–692.
(32) Moad, G.; Rizzardo, E.; Thang, S. *Aust. J. Chem.* **2005**, *58*, 379–410.
(33) Evans, R. A.; Hanley, T. L.; Skidmore, M. A.; Davis, T. P.; Such, G. K.; Yee, L. H.; Ball, G. E.; Lewis, D. A. *Nat. Mater.* **2005**, *4*, 249–254.
(34) Evans, R. A.; Hanley, T. L.; Skidmore, M. A.; Yee, L. H.; Lewis, D. A. Photochromic Compositions and Light Transmissible Articles. WO 2004/041961 A1, 2003.
(35) Such, G.; Evans, R. A.; Yee, L. H.; Davis, T. P. *J. Macromol. Sci., Polym. Rev.* **2003**, *C43*, 547–579.
(36) Such, G. K.; Evans, R. A.; Davis, T. P. *Macromolecules* **2004**, *37*, 9664–9666.
(37) Such, G. K.; Evans, R. A.; Davis, T. P. *Mol. Cryst. Liq. Cryst.* **2005**, *430*, 273–279.
(38) Such, G. K.; Evans, R. A.; Davis, T. P. *Macromolecules* **2006**, *39*, 1392–1396.
(39) Such, G. K.; Evans, R. A.; Davis, T. P. *Macromolecules* **2006**, *39*, 9562–9570.
(40) Malic, N.; Campbell, J. A.; Evans, R. A. *Macromolecules* **2008**, *41*, 1206–1214.
(41) Sriprom, W.; Néel, M.; Gabbutt, C. D.; Heron, M.; Perrier, S. *J. Mater. Chem.* **2007**, *17*, 1885–1893 .
(42) Evans, R. A.; Such, G. K.; Malic, N.; Davis, T. P.; Lewis, D. A.; Campbell, J. A. Photochromic Compounds Comprising Polymeric Substituents and Methods for Preparation and Use Thereof. WO/2006/024099, **2006**.
(43) Gabbutt, C. D.; Hepworth, J. D.; Heron, M.; Thomas, D. A.; Partington, S. M. *Heterocycles* **2004**, *63*, 567–582.
(44) Gabbut, C. D.; Heron, B. M.; Instone, A. C.; Horton, P. N.; Hursthouse, M. B. *Tetrahedron* **2005**, *61*, 463–471.
(45) Chamontin, K.; Lokshin, V.; Rossolin, V.; Samat, A.; Guglielmetti, R. *Tetrahedron* **1999**, *55*, 5821–5830.
(46) Tanaka, K.; Aoki, H.; Hosomi, H.; Ohba, S. *Org. Lett.* **2000**, *2*, 2133–2134.
(47) DiNunzio, M. R.; Gentili, P. L.; Romani, A.; Favaro, G. *ChemPhysChem* **2008**, *9*, 768–775.
(48) Jockusch, S.; Turro, N.; Blackburn, F. *J. Phys. Chem. A.* **2002**, *106*, 9236–9241.
(49) Kumar, A.; Van Gemert, B.; Knowels, D. Novel Substituted Naphthopyrans, WO/1995/16215, **1995**.
(50) Haddleton, D. M.; Jasieczek, C. B.; Hannon, M. J.; Shooter, A. J. *Macromolecules* **1997**, *30*, 2190–2193.
(51) Biteau, J.; Chaput, F.; Boilot, J. *J. Phys. Chem.* **1996**, *100*, 9024–9031.
(52) Zayat, M.; Levy, D. *J. Mater. Chem.* **2003**, *13*, 727–730.
(53) Pozzo, J. L.; Samat, A.; Guglielmetti, R.; De Keukeleireb, D. *J. Chem. Soc., Perkin Trans. 2* **1993**, 1327–1332.
(54) Pozzo, J. L.; Samat, A.; Guglielmetti, R.; Dubest, R.; Aubard, J. *Helv. Chim. Acta* **1997**, *80*, 725–738.
(55) Babazadeh, M. *J. App. Polym. Sci.* **2006**, *102*, 4989–4995.
(56) Gauglitz, G. Ch. 2, Photophysical, Photochemical, and Photokinetic Properties of Photochromic Systems. In *Photochromism: Molecules and Systems*, rev. ed.; Dürr, H., Bouas-Laurent, H., Eds.; Elsevier: Amsterdam, 2003; pp 15−61.
(57) Favaro, G.; Malatesta, V.; Mazzucato, U.; Ottavi, G.; Romani, A. *J. Photochem. Photobiol., A* **1995**, *87*, 235–241.
(58) Haddleton, D. M.; Kukulj, D.; Duncalf, D. J.; Heming, A. M.; Shooter, A. J. *Macromolecules* **1998**, *31*, 5201–5205.
(59) Sallenave, X.; Delbaere, S.; Vermeersch, G.; Saleh, A.; Pozzo, J.-L. *Tetrahedron Lett.* **2005**, *46*, 3257–3259.
(60) Beuermann, S., Jr.; Mc Minn, J. H.; Hutchinson, R. A. *Macromolecules* **1996**, *29*, 4206–4215.

MA801947D